European Journal of Neuroscience, Vol. 23, pp. 83–93, 2006 doi:10.1111/j.1460-9568.2005.04539.x

Neurogenic niche modulation by activated microglia: transforming growth factor β increases neurogenesis in the adult dentate gyrus

Daniela Battista,[1] Carina C. Ferrari,[1] Fred H. Gage[2] and Fernando J. Pitossi[1]
[1]Laboratory of Neuromodulation, Leloir Institute, CONICET-UBA, University of Buenos Aires, 435 Av Patricias Argentinas, Buenos Aires 1405, Argentina
[2]Salk Institute, San Diego, USA

Keywords: cytokine, inflammation, microglia, neuron, proliferation, stem cells

Abstract

Adult neural stem cells (NSC) proliferate and differentiate depending on the composition of the cellular and molecular niche in which they are immersed. Until recently, microglial cells have been ignored as part of the neurogenic niche. We studied the dynamics of NSC proliferation and differentiation in the dentate gyrus of the hippocampus (DG) and characterized the changes of the neurogenic niche in adrenalectomized animals (ADX). At the cellular level, we found increased NSC proliferation and neurogenesis in the ADX animals. In addition, a morphologically distinct subpopulation of NSC (Nestin+/GFAP–) with increased proliferating profile was detected. Interestingly, the number of microglial cells at stages 2 and 3 of activation correlated with increased neurogenesis ($r^2 = 0.999$) and the number of Nestin-positive cells ($r^2 = 0.96$). At the molecular level, transforming growth factor beta (TGF-β) mRNA levels were increased 10-fold in ADX animals. Interestingly, TGF-β levels correlated with the amount of neurogenesis detected ($r^2 = 0.99$) and the number of stage 2 and 3 microglial cells ($r^2 = 0.94$). Furthermore, blockade of TGF-β biological activity by administration of an anti-TGF-β type II receptor antibody diminished the percentage of 5-bromo-2′-deoxyuridine (BrdU)/PSA-NCAM-positive cells *in vivo*. Moreover, TGF-β was able to promote neurogenesis in NSC primary cultures. This work supports the idea that activated microglial cells are not pro- or anti-neurogenic *per se*, but the balance between pro- and anti-inflammatory secreted molecules influences the final effect of this activation. Importantly, we identified an anti-inflammatory cytokine, TGF-β, with neurogenic potential in the adult brain.

Introduction

In the adult brain, two areas retain the capacity to generate new neurons from adult stem/progenitor cells (NSC); the subgranular zone of the dentate gyrus (DG) and the subventricular zone of the lateral ventricle wall (Gage, 2002). NSC proliferation and differentiation towards a specific phenotype are regulated by the characteristics of the environment or niche in which they reside (Gage, 2002; Alvarez-Buylla & Lim, 2004). This niche is composed of neighbouring cells as well as soluble and membrane-bound factors and the extracellular matrix. The dynamics of the changes in composition of this niche and the key factors regulating neurogenesis are currently being elucidated.

Microglial cells are the main cellular component of the CNS of nonectodermal origin. They become activated after changes in the milieu by altering their morphology and the pattern of secreted factors such as immune cytokines (Perry *et al*., 2003). Immune cytokines play a plethora of modulating roles in the central nervous system in dissimilar processes, such as immune-mediated responses, long-term potentiation and neuronal survival or demize (Besedovsky & del Rey, 1996). Until recently, microglial cells have been ignored as part of the environment that could affect the proliferation and differentiation of NSC. Only recently, CNS inflammation has been associated with inhibition of neurogenesis (Vallieres *et al*., 2002; Ekdahl *et al*., 2003; Monje *et al*., 2003). As immune cytokines are synthesized not only after brain injury or cellular transplantation but also under physiological conditions in the brain, it is relevant to study their role in modifying the neurogenic niche.

Pro-inflammatory cytokine functions are physiologically down-regulated mainly by two mechanisms. The first relies on the expression of anti-inflammatory cytokines, such as IL-1ra and TGF-β (Dinarello, 1996). The balance between pro- and anti-inflammatory cytokines can modulate the final effect of the cytokines in the inflammatory reaction. Recently, IL-6, a pro-inflammatory cytokine, has been shown to have anti-neurogenic effects (Vallieres *et al*., 2002; Monje *et al*., 2003). Whether anti-inflammatory cytokines play a role in the regulation of the neurogenic niche remains unknown. The second physiological mechanism of regulation of cytokine action is mediated by glucocorticoids (GC; Dinarello, 1996). Cytokine release in the periphery activates the hypothalamus-pituitary-adrenal axis, liberating GC that down-regulate cytokine actions also in the brain (Besedovsky *et al*., 1986).

In parallel, deprivation of GC by adrenalectomy results in apoptotic cell death (mainly of older neurons) and increased NSC proliferation, specifically in the DG (Sloviter *et al*., 1989; Gould *et al*., 1992; Cameron & Gould, 1994; Cameron & McKay, 1999; Montaron *et al*., 1999). Still, other factors that alter the neurogenic niche to promote NSC proliferation and differentiation cannot be discarded.

Correspondence: Dr Fernando J. Pitossi, as above.
E-mail: fpitossi@leloir.org.ar

Received 3 May 2005, revised 3 November 2005, accepted 8 November 2005

In this study, we sought to characterize the neurogenic niche of the DG at the cellular and molecular levels in animals deprived of their adrenal gland as a model to identify factors modulating neurogenesis. This approach allows a better dissection of the functional role of the activated microglia in modulating neurogenesis and points to an anti-inflammatory cytokine, TGF-β, as a key factor in neurogenesis.

Materials and methods

Surgery, BrdU injections and tissue treatment

Adult male Wistar rats (200 g to 250 g; Iname, Buenos Aires) were bilaterally adrenalectomized (ADX) or sham-operated (Sham) under ketamine chlorhydrate (80 mg/kg) and xylazine (8 mg/kg) anaesthesia. ADX animals were given a saline drinking solution. All surgical procedures took place during the morning to avoid circadian variations, and subjects were first acclimatized to the colony for one week. Standard rat chow and water were freely available. During the three days after surgery, animals were injected intraperitoneally with 5-bromo-2′-deoxyuridine (BrdU, Sigma-Aldrich, MA, USA; 50 mg/kg body weight dissolved in 0.1 M NaOH, 0.9% NaCl) once each day 2 h after the beginning of the light period. On the fourth day, animals were deeply anaesthetized and perfused transcardially with heparinized saline. Brains were removed and hippocampi from the right hemispheres were immediately frozen in liquid nitrogen for further RNA extraction. Left hemispheres were postfixed overnight at 4 °C in 4% paraformaldehyde in 0.1 M phosphate buffer (PB), after which they were cryoprotected in 30% sucrose in PB and sliced coronally in 40-μm sections with a sliding cryostat. Slices were stored at −20 °C in 30% glycerol, 30% ethylene glycol and 40% PB.

For TGF-β receptor blockade, ADX and Sham-operated animals were anaesthetized and injected unilaterally (right hemisphere) the day after the surgery with a rabbit antibody against type II TGF-β receptor (α-TGFR 200 ng/μL Santa Cruz Biotechnology, Santa Cruz, CA, sc-400) or normal rabbit IgG (control 200 ng/μL Santa Cruz, sc-2027; Boche *et al*., 2003). The stereotaxic injections were performed with a 50-μm tipped fine glass capillary directed to the right DG at bregma, antero-posterior, −3.8 mm; lateral, −1.5 mm; ventral, −3.3 according to Paxinos (1986). One microlitre of the solution was infused over a 7-min period. BrdU injections and perfusion were performed as described above except that both hemispheres were cryoprotected and sliced as previously described. Animal procedures were performed according to the rules and standards of the German animal protection law and the regulations for the use of laboratory animals of the National Institutes of Health, USA.

Radioimmunoassay

A radioimmunoassay against plasma corticosterone was performed from trunk blood collected before perfusion. Antibody against corticosterone was purchased from Sigma (C8784) and ^{3}H-corticosterone from NEN (NEN Life Science Products, Inc., NET399). The assay was carried out following RIA protocol from the Anti-corticosterone data sheet. Serum samples were diluted 1 : 10 in buffer B (0.05 M NaBorate pH 7.8, 0.02% NaAzide, 0.25% BSA) to a final volume of 200 μL, extracted with 700 μL of ether and resuspended in 100 μL of buffer B before the assay. All ADX rats displayed corticosterone levels below 0.01 μg/mL.

RNA isolation, reverse transcription and RT-PCR

Total RNA was prepared by homogenizing hippocampal tissue in 500 μL of guanidinium thiocyanathe solution (4 M guanidinium thiocyanathe, 25 mM sodium citrate pH 7, 0.5% sarcosyl, 0.1 M 2-mercaptoetanol), 50 μL 2 M sodium citrate pH 4 and 500 μL phenol saturated in water as described before (Depino *et al*., 2003). Polyinosinic acid (1 μL) was added as a carrier and the mixture was extracted with 100 μL of chloroform/isoamyl alcohol solution (49 : 1). The aqueous phase was precipitated with 500 μL isopropanol and resuspended in 20 μL of RNAse-free milliQ water. Samples were treated with DNAse (Invitrogen, San Diego, CA) and reverse transcription was performed by incubating 10 μL of the DNAse-treated RNA with 1 μL oligo-dT (Amersham Pharmacia Biotech, Buckinghamshire, UK) and 5 μL SuperScript First-strand Synthesis System for RT-PCR (Invitrogen), according to manufacturer's protocol.

For quantitative real time PCR reaction, 21 μL SYBR Green Master Mix was added to 100–500 ng cDNA. The SYBR Green Master Mix consisted of: 3 M $MgCl_2$, 1 μL of 10× PCR buffer, 0.3 mM dNTPs, 0.1 mM fluorescein, 0.1 mM BSA, 0.4 μL of 1000 × SYBR Green (Molecular Probes), 20 μM taq plathinium (Invitrogen, Life Technologies) and 1 μL of either β2-microglobulin, IL-1α, IL-1β, IL1-ra, TGF-β or TNF-α forward and reverse primers (4 μM). Quantitative RT-PCR was performed on a iCycler IQ^{TM} Real Time PCR Detection System, Bio-Rad. Reaction conditions were as follows: 1 min at 95 °C, 42 cycles of 30 s at 95 °C, 1 min at 56 °C, 0.45 s at 72 °C and 10 s at 82 °C. The specificity of PCR primers was tested, and a single DNA band of the expected molecular size was observed in a 1% agarose gel electrophoresis stained with ethidium bromide. In addition, a single peak in the iCycler plot was observed after a melting curve was performed. Reverse and forward primers are summarized in Table 1. Each sample was tested in triplicate. To compare cytokine mRNA expression between treatments, the amount of cytokine was expressed as the ratio of cytokine/β_2-microglobulin levels.

Immunohistochemistry and immunofluorescent staining

For BrdU staining alone, one-in-six series of free-floating sections were blocked for peroxidase activity with 3% hydrogen peroxide in methanol. Slices were then incubated for 2 h in 50% formamide at

TABLE 1. Primers sequences used for RT-PCR

	Forward primer	Reverse primer	Amplicon (pb)
β2	TCTTTCTGGTGCTTGTCTC	AGTGTGAGCCAGGATGTAG	241
IL-1β	TCCATGAGCTTTGTACAAGG	GGTGCTGATGTACCAGTTGG	237
IL-1α	AACTGGCTCAGTCTTTTGCC	TTGTGACACCCTGGTTTGAG	207
IL-1rα	GACCCTGCAAGATGCAAGCC	AGAGGAACCATCCTGGACAG	349
TGF-β1	ACCAACTACTGCTTCAGCTC	TGTTGGTTGTAGAGGGCAAG	189
TNF-α	AAATGGGCTCCCTCTCATCA	AGCCTTGTCCCTTGAAGAGA	248

65 °C, washed once in 2× standard saline citrate (SSC; 0.3 M NaCl, 0.03 M sodium citrate), incubated for 30 min at 37 °C in 2 M HCl, rinsed in 0.1 M borate buffer, pH 8.5, and thoroughly washed in Tris-buffered saline (TBS; Tris-HCl 50 mM pH 7.4, NaCl 150 mM). Sections were blocked in 0.1% Triton X-100, 1% donkey serum in TBS (blocking solution) for 40 min at room temperature (RT). Mouse monoclonal IgG anti-BrdU (1 : 200; Boehringer Mannheim-Roche, Indianapolis, IN, USA) was diluted in blocking solution and sections were incubated for 48 h at 4 °C. Sections were then incubated in biotin-labelled donkey anti-mouse IgG (1 : 200; Jackson Laboratories, West Grove, PA, USA) for 2 h at room temperature (RT) followed by the Vectastain standard ABC kit (Vector, Burlingame, CA, USA). 3–3′Diaminobenzidine (DAB, 0.5 mg/mL; Sigma) was used as a chromogen and sections were mounted in DPX (Fluka, Buchs, Switzerland).

For double Brdu/GFAP (astrocytic proliferation) and BrdU/GSA (microglial proliferation) immunofluorescence, sections were incubated in mouse anti-BrdU as previously described and in either rabbit anti-glial fibrillary acidic protein (GFAP, 1 : 500; Chemicon, Temecula, CA, USA) or biotinylated *Griffonia simplicifolia* lectin I isolectin B4 (GSAI-B4, 1 : 100; Vector) antibodies. GSAI-B4 was used to assess microglial activation based on GSA1-B4 positive stain and cell morphology (Kreutzberg, 1996). Three stages of microglial activation were defined. Stage 1 cells had rod-shaped cell bodies with fine, ramified processes and were defined as resting microglial cells. Stage 2 cells had elongated cell bodies with long thick processes, and stage 3 cells had small, thick processes and a rounded morphology with vacuolated cytoplasm. Stages 2 and 3 were defined as activated microglial cells.

For double BrdU/Nestin (stem cell proliferation) and BrdU/PSA-NCAM (neurogenesis) staining, a rat anti-BrdU (1 : 150; Abcam, Cambridge, UK) and a mouse anti-Nestin (1 : 200; BD Biosciences-Pharmigen) or a mouse anti-PSA-NCAM (1 : 150; generous gift from Dr Seki) were used. For double immunofluorescence staining for GFAP/Nestin, the same antibodies as described previously were used. Three types of Nestin-positive cells were classified according to cell morphology and double-labelling with GFAP. Type 1 cells had long, thin processes along the granular cell layer (GCL) and were sometimes stained positive for GFAP. Type 2 cells had rounded cell bodies and were mainly located towards the subgranular cell layer (SGZ). Type 3 cells had small processes, tangential to the GCL. This classification has some similarities to the Nestin-positive cell population described by Kronenberg *et al*. (2003). Type 2 and type 3 Nestin-positive cells were GFAP-negative. Double immunofluorescence staining for GSAI-B4/ED1 (1 : 100; Serotec, Kidlington, Oxford, UK) was also performed to assess phagocytic microglial cells.

Secondary antibodies used were Cy3-conjugated donkey anti-mouse, Cy2-conjugated donkey anti-rabbit, Cy3 donkey anti-rabbit and biotin-conjugated donkey anti-rat and Cy2- and Cy3-conjugated streptavidin (1 : 200; Jackson). Sections were mounted in Mowiol (Calbiochem, La Jolla, CA, USA).

For double TGF-β1/GSAI-B4 immunohistochemistry a rabbit anti-TGF-β1 (1 : 25; Santa Cruz) antibody together with the previously described GSAI-B4 antibody were used. Sections were incubated with primary antibodies 48 h at 4 °C, then incubated with peroxidase-conjugated donkey anti-rabbit (1 : 200; Jackson) for 2 h at RT and further treated 5 min with DAB. After the immunohistochemistry for TGF-β1 was completed, sections were blocked for peroxidase activity for 20 min with 3% hydrogen peroxide in PB, washed and incubated with the Vectastain standard ABC kit as described before. Vector NovaRed (Vector, SK-4800) was used as a chromogen. Sections were mounted in DPX (Fluka, Buchs, Switzerland).

Cresyl violet staining was also performed to assess inflammatory infiltrate cells and apoptotic nuclei, as described by (Ferrari *et al*., 2004).

Cell culture and immunocytochemistry

Adult hippocampal precursor cells were prepared from adult male Wistar rats (4–6 weeks old). Hippocampi were dissected and dissociated in PPD solution (2.5 U/mL papain, Worthington Biochemical Corporation; 1 U/mL dispase II, Boehringer Mannheim-Roche; 250 U/mL Dnase I Worthington in PBS-Glucose, Gibco, Life Technologies) at 37 °C for 15 min, gently triturated and then incubated for another 20 min at 37 °C. Cells were washed in DMEM/F12 medium with 10% of fetal bovine serum (FBS, HyClone, Logan, UT) and mixed with PBS-equilibrated Percoll solution (9 mL Percoll : 1 mL PBS 10×). The cell suspension was fractionated by centrifugation for 30 min at 18 °C at 20 000 × *g*. The cell pellet was washed twice with DMEM/F12 medium and plated on poly-L-ornithine- (Sigma)/laminin (BD Biosciences-Clontech) coated dishes (Palmer *et al*., 1999) in DMEM/F12 supplemented with N2 (Gibco) and antibiotic/antimicotic solutions (Gibco) (standard medium) with 10% FBS and 20 ng/mL of human recombinant FGF-2 (Peprotech, DF, Mexico). Twenty-four hours later, medium was replaced with serum-free standard medium with 20 ng/mL of FGF-2. All experiments were performed after passage 15.

For differentiation experiments, 0.35×10^5/mL cells were plated on poly-L-ornithine/laminin-coated cover slides. Two days after replication, differentiation medium (standard medium with 0.5 ng/mL FGF, 0.5 nM FSK and 1% fetal bovine serum) or standard medium with a low FGF concentration (low FGF, 0.5 ng/mL FGF) was added with or without 1 ng/mL of TGF-β1 (Peprotech). Medium was changed every two days and, on the seventh day after replication, cells were fixed in 4% paraformaldehyde for 10 min at 4 °C.

For proliferation experiments, 0.35×10^5/mL cells were plated on poly-L-ornithine/laminin-coated cover slides. Two days after replication, medium was changed to fresh standard medium supplemented with 20 ng/mL FGF and 20 nM BrdU (Sigma). One hour after the BrdU pulse, fresh medium without BrdU and with or without 5 ng/mL of TGF-β1 was added. Twenty-four hours later, cells were fixed as described previously.

As a control, 10 μg/mL of a TGF-β1 neutralizing antibody (Ab) was added (R & D systems, UK; Farkas *et al*., 2003). All treatments were performed in triplicate and three independent experiments were performed.

For Tuj I, GFAP and Nestin immunofluorescence, fixed cells were blocked for 30 min in 0.1% Triton X-100, 1% donkey serum in PBS and then incubated in either mouse anti-type III β-tubulin (Tuj I, 1 : 1000, Promega Corporation, Madison, USA), rabbit anti-GFAP (1 : 1000; Chemicon) or mouse anti-Nestin (1 : 1000; Pharmigen) for 2 h at RT. Cells were then washed three times with PBS and incubated in secondary antibodies for 2 h at RT. The percentage of positively stained cells over the total number of cells was counted for each marker.

To assess cell proliferation after TGF-β1 treatment, double immunofluorescence for BrdU/PCNA was performed. Briefly, cells were treated with 2 M HCl for 30 min at RT, rinsed in 0.1 M borate buffer, pH 8.5, washed twice with PBS, blocked for 30 min at RT and incubated with rat anti-BrdU (1 : 800; Abcam) and mouse anti-PCNA (1 : 800; Novocastra Laboratories, Newcastle, UK) for 2 h at RT. Cells were then washed three times in PBS and incubated in secondary antibodies for 2 h at RT. The percentage of double-labelled cells over

the total of BrdU-positive cells was counted. PCNA-positive stain is indicative of cells that are dividing at the time of fixation. Double-labelled cells were counted to assess which cells that were dividing at the time of the BrdU pulse (BrdU-positive) were still dividing 24 h after the treatment with TGF-β1 (double-labelled cells).

Secondary antibodies used were Cy3-conjugated donkey anti-mouse, Cy2-conjugated donkey anti-rat and Cy2-conjugated donkey anti-rabbit (1 : 1000; Jackson). Cell nuclei were stained with Hoescht (Sigma) and mounted with Mowiol (Calbiochem).

Quantification and imaging

One-in-six series of coronal sections (40-μm thick) from the entire hippocampus (−2.56 mm to −5.2 mm from bregma) were stained for BrdU using DAB immunohistochemistry and counterstained with eosin. BrdU-labelled cells in the GCL and the SGZ were quantified at 40× magnification under a light microscope. The total number of positive cells through the entire GCL was estimated and then divided by the volume of the DG. This volume was calculated using the Image Pro image analysis system (Media Cybernetics, Silver Spring, MD). When Brdu-positive cells were counted in the animals injected with the antibodies, only the sections around the site of the injection were taken into account (−3.14 mm to −4.3 mm from bregma).

For Nestin- and Nestin/GFAP-positive cells quantification, three to six coronal sections were analysed at 40× magnification under a fluorescence microscope (Nikon eclipse, e600), and the average of cells per section was calculated. For GSA1-B4 quantification, one-in-12-series of the coronal sections through the entire GCL were analysed under a fluorescence microscope and divided by the volume of the DG. To estimate the number of apoptotic cells, one-in-12-series of the coronal sections were stained with cresyl violet as in (Ferrari *et al*., 2004) and apoptotic nuclei were counted.

Double-stained cells in the GCL were quantified using *z*-scan confocal microscopy (Zeiss LSM 510 confocal-laser scanning microscope equipped with an argon and He/Ne laser that emitted at 488 nm and 568 nm, respectively) at 40× magnification. Each cell was analysed along the entire '*z*' axis. Between 40 and 100 BrdU-positive cells were counted to calculate double-labelled cell percentages, and the total number of double-labelled cells was estimated.

Cell culture analysis was performed at 40× magnification under a fluorescent microscope. Approximately 400 cells were counted for each cover slide using the Image Pro image analysis system.

Statistical analysis

Data are presented as the mean ± standard error of the mean (SEM). Comparisons were performed using Student's *t*-test (two-tailed) and one-way analysis of variance (ANOVA) followed by *posthoc* Tukey test or Dunett test. Differences were considered significant at $*P \leq 0.05$; $**P \leq 0.01$; $***P \leq 0.001$. Data were transformed when necessary to fulfil normality and homocedacy criteria. For correlation analysis, a linear regression was performed (r^2; correlation coefficient, slope was considered significantly different from zero at $*P \leq 0.05$).

Results

Characterization of the increased cell proliferation in the DG of the hippocampus caused by adrenalectomy

Male Wistar rats were bilaterally adrenalectomized (ADX), checked for the efficiency of the adrenalectomy by quantifying corticosterone levels by RIA, injected with BrdU for 3 days and analysed 1 day later as described in Materials and methods (Fig. 1A). Adrenalectomy caused a dramatic increment in the number of apoptotic cells along the DG (Fig. 1B). The removal of the adrenal glands also augmented the number of BrdU+ proliferating cells in the DG (nearly three-fold increase between ADX and Sham-treated animals; Fig. 1C and D).

The increment in BrdU+ cells was reflected in statistically significant proliferation of NSC (defined as BrdU and Nestin double-positive cells) and newborn neurons (defined as BrdU and PSA-NCAM double-positive cells) but not GFAP+ cells ($*P < 0.05$, $***P < 0.001$, $P = 0.23$, respectively, Fig. 1E–J). The percentage of proliferating NSC in the SGZ of the DG increased more than three-fold in ADX rats in comparison to the Sham-treated animals ($*P < 0.05$, Fig. 1E and F). In addition, the percentage of BrdU/PSA-NCAM positive cells increased by 12% in ADX compared to control animals and represented 75% of all proliferating cells in ADX rats ($**P < 0.01$, Fig. 1G and H). Because of this high proportion of BrdU cells expressing also PSA-NCAM, when the number of proliferating, BrdU/PSA-NCAM cells was calculated as the total number of double labelled cells per mm^3 of dentate gyrus, this cell population increased three-fold between Sham and ADX animals (44 ± 6 vs. 136 ± 10, respectively) The percentage of BrdU/GFAP double-positive cells did not increase significantly with ADX ($P = 0.56$, Fig. 1I and J).

Characterization of the NSC population

As different subpopulations of NSC seem to be related to the renovation of the NSC pools and in the different steps of the differentiation process, we further characterized the NSC populations along the DG and their dynamics during adrenalectomy. The total number of Nestin/GFAP-double-positive cells did not change significantly (Fig. 2A). Nestin-positive cells were classified according to morphology into three subgroups using criteria similar to those used by Kemperman and colleagues with subtle modifications (see Materials and methods; Fig. 2B–E) (Kronenberg *et al*., 2003) The number of Nestin+ cells of each subgroup was estimated throughout the entire SGZ. Some of the type 1 Nestin+ colabelled with GFAP (Fig. 2E) whereas type 2 and type 3 Nestin+ cells stained negative for GFAP (Fig. 2C and D). Only an increased number of type 2 Nestin+/GFAP– cells was found in adrenalectomized rats compared with Sham-operated animals. No such increase was detected in type 1 and 3 Nestin-positive cells ($**P < 0.001$, Fig. 2A).

Characterization of the cellular environment of the DG after ADX. Stage 2 and 3 microglial activation correlates with neurogenesis and NSC proliferation after ADX

As no morphological modifications or net change in the number of astrocytes (Fig. 1J) were detected in ADX animals compared to controls, we focused our analysis on microglial reaction to ADX. Microglial cells in the DG were found to be activated at different stages, according to cell morphology (Fig. 3A–D). Microglial activation was found in no other brain region, included the subventricular zone, another neurogenic area (data not shown). The number of activated microglial cells (stage 2 and 3, see Materials and methods) increased at least eight-fold after ADX ($*P < 0.05$, Fig. 3D). These microglial cells were not fully activated to a macrophagic phenotype, as no ED-1+ cell could be detected (data not shown). Microglial proliferation was evident in ADX rats (Fig. 3C). Indeed, the percentage of dividing microglia (BrdU/GSAI-B4-positive cells)

over the total number of proliferating cells increased from 3.9% to 15.5% in Sham and ADX rats, respectively. In addition, no immune cell recruitment from the periphery could be observed in any animal examined by Cresyl violet staining (data not shown). Thus, as expected for an apoptotic cell death, no inflammation with peripheral immune cell infiltration was observed (Depino *et al*., 2003). Also typically, a distinct type of microglial activation was detected that did not proceed to full macrophagic (ED-1) activation.

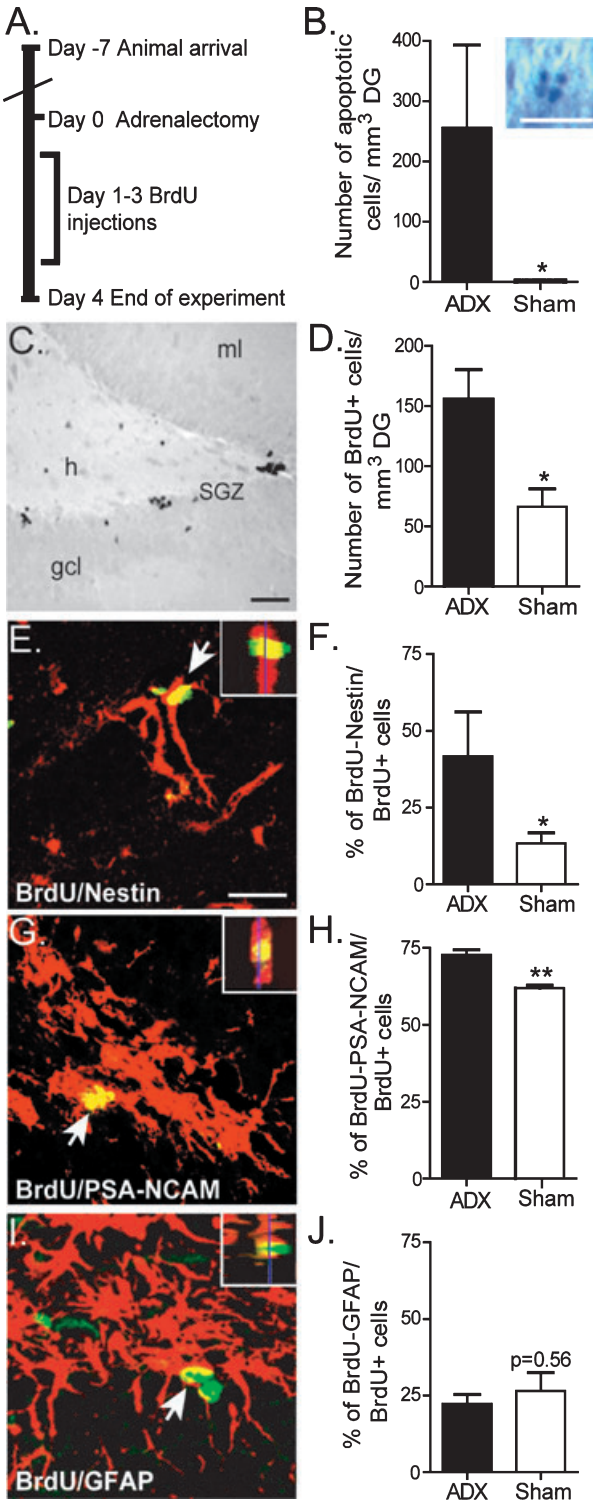

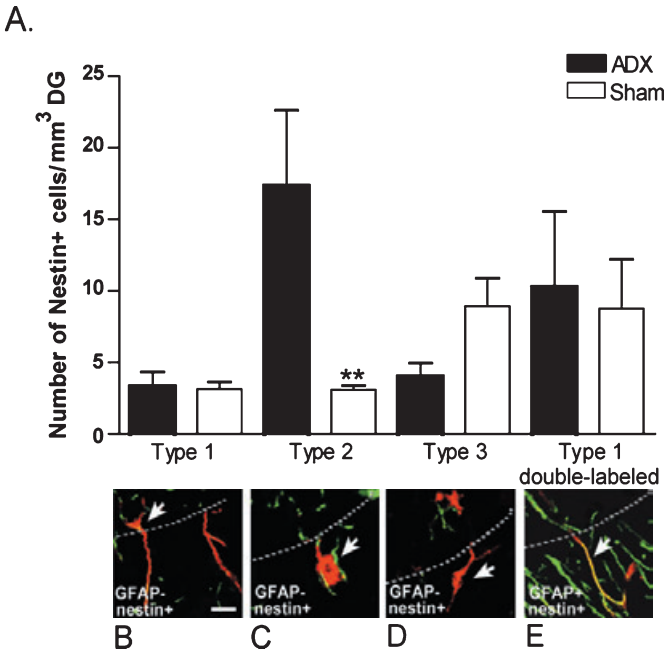

FIG. 2. Type 2 Nestin-positive, GFAP negative cell population proliferates with ADX. (A) Quantification of the number of Nestin/GFAP-positive cells in the GCL. (B–E) Representative photomicrographs of Nestin (red) and GFAP (green) immunofluorescence showing different cell morphologies. Nestin-positive cells were classified in four types according to their morphology and double-labelling with GFAP (see Material and methods). Arrows indicate positive cells; dotted line outlines the subgranular cell layer of the DG. Values are the mean ± SEM (Student's *t*-test between treatments for each cell type. $^{**}P < 0.05$. ADX $n = 5$, Sham $n = 6$). Scale bar, 20 μm.

Biological variation was observed in the degree of NSC proliferation, neurogenesis and microglial activation of each animal. Interestingly, only stage 2- and 3-activated microglial cell numbers, but not resting microglia (stage 1), correlated with the number of BrdU/PSA-NCAM double-positive cells and the augmented population (type 2) of Nestin-positive cells after ADX ($r^2 = 0.999$ and 0.96, respectively, Fig. 3E and F).

FIG. 1. Adrenalectomy (ADX) increases apoptosis, neural stem cell (NSC) proliferation, and neurogenesis. (A) Timeline of the experimental approach. (B–J) Analysis of the BrdU-positive cell population and apoptosis in ADX and Sham-operated (Sham) animals. (B) Quantification of the total number of apoptotic cells in the granule cell layer (GCL)/mm^3 of the dentate gyrus (DG) of ADX and Sham-operated animals. (Inset) Cresyl violet staining showing an apoptotic nucleus. ADX significantly increases apoptosis ($^*P < 0.05$, data were transformed; log *x*). (C) Immunohistochemistry of a representative section of the DG showing BrdU-positive cells. (D) Number of BrdU-positive cells in the GCL/mm^3 DG for both treatments. ADX significantly increases cell proliferation ($^*P < 0.05$). (E–J) Confocal *z*-scanning analysis of BrdU double-labelled cells in the GCL. (E, G, and I) Immunofluorescence of representative sections of the DG showing BrdU (green) and different cell markers (red) positive cells. (E) BrdU/Nestin (G) BrdU/PSA-NCAM (I) BrdU/GFAP-positive cells. Arrows indicate double-labelled cells. (Insets) *z*-axis showing double-labelled cells. Quantification of the percentage of double-labelled cells in the SGZ among the BrdU-positive cell population for both treatments. (F) BrdU/Nestin ; (H) BrdU/PSA-NCAM ; (J) BrdU/GFAP–double-positive cells. ADX significantly increases NSC proliferation ($^*P < 0.05$, data were transformed; $\sqrt{x}$) and neurogenesis ($^{**}P < 0.01$) but not the number of BrdU/GFAP-positive cells ($P = 0.56$). h, hilus; gcl, granule cell layer; ml, molecular layer; sgz, subgranular zone. Values are the mean ± SEM (Student's *t*-test; ADX $n = 5$, Sham $n = 6$). Scale bar, 20 μm (B, E, G, I and K); 50 μm (C).

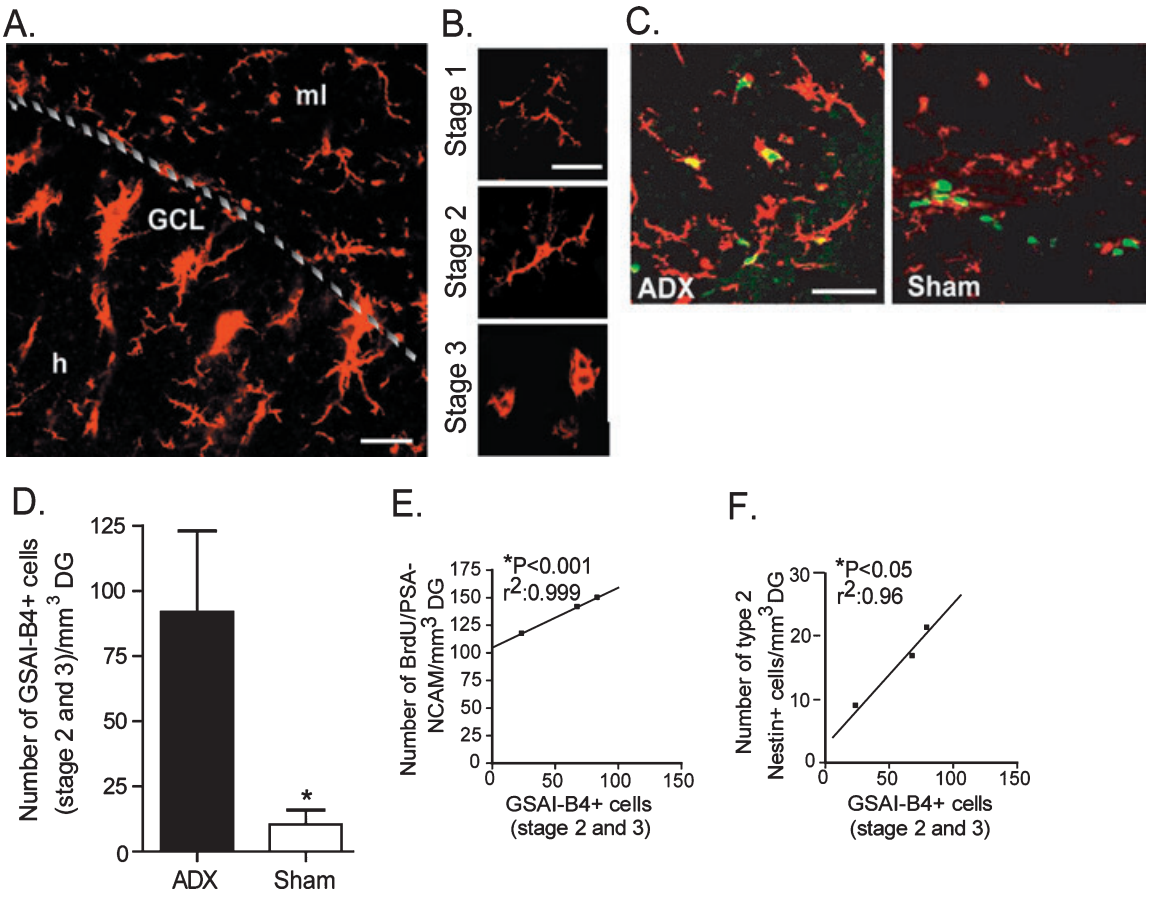

FIG. 3.

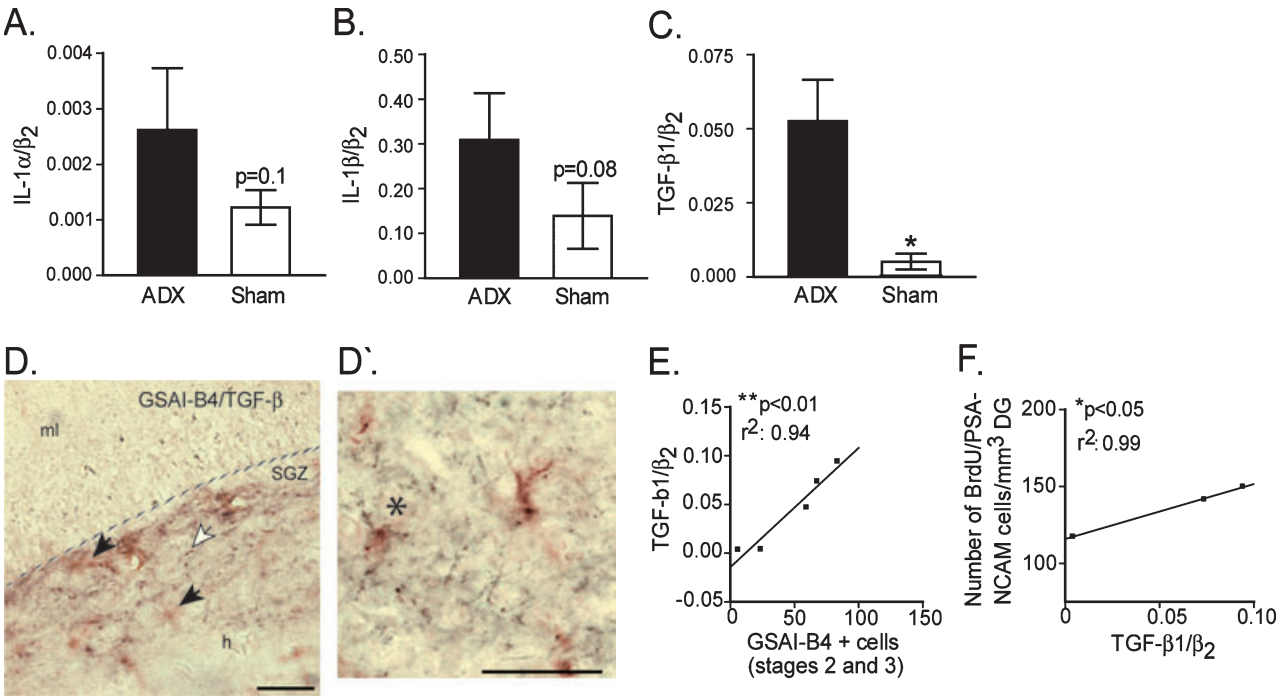

FIG. 4.

Characterization of the cytokine profile in the DG of ADX rats: correlation between neurogenesis, microglial activation and TGF-β expression

Microglial activation and its effects on their surroundings depend mainly on the profile of secreted factors. Thus, we sought to characterize the expression profile of key cytokines in this area by real-time PCR in the hemisphere contralateral to the one subjected to previous analysis. Very modest increments in pro-inflammatory cytokines such as interleukin-1 (IL-1) α and IL-1β were detected in this area, but they did not achieve statistical significance (Fig. 4A and B). Interestingly, a ten-fold increase in transforming growth factor-beta (TGF-β1) expression was detected and reached statistical significance (*$P < 0.05$, Fig. 4C and D). Tumor necrosis factor alpha and IL-1ra mRNAs were not detected in the hippocampus of any animal studied (data not shown). TGF-β1 immunoreactivity was observed specifically in the hippocampus and not in other brain regions of adrenalectomized rats (Fig. 4D and data not shown). TGF-β1 expression was detected in microglial cells by colocalization with the microglial cell marker GSAI-B4 (Fig. 4D and D′).

When individual variations were considered, TGF-β1 ($r^2 = 0.94$), but not IL-1α ($r^2 = 0.12$), or IL-1β ($r^2 = 0.42$) mRNA levels, correlated with stage 2- and 3-activated microglial cells (Fig. 4E and data not shown). Interestingly, TGF-β1 mRNA levels correlated equally well with the number of newborn neurons in ADX rats (Fig. 4F, $r^2 = 0.99$).

The neurogenic effect of adrenalectomy is partially mediated by TGF-β

To test the hypothesis that TGF-β expression levels and neurogenesis were functionally related, ADX and Sham-operated animals were injected with an antibody against the type II TGF-β receptor or control antiserum in the DG 1 day after surgery. This antibody has been shown to neutralize TGF-β bioactivity specifically *in vivo* (Boche *et al*., 2003).

TGF-β neutralization had no effect on the total number of proliferating cells in ADX or Sham-operated animals (Fig. 5A). Again, the nearly three-fold induction in the number of BrdU positive cells after ADX can be observed (Fig. 5A). Interestingly, there was an estimated 30% reduction in the percentage of BrdU/PSA-NCAM double-positive cells among the total proliferating cell population in ADX rats treated with the anti-type II TGF-β receptor, but not in control-treated ADX animals (Fig. 5B). The anti-TGF-β treatment in ADX rats returned the percentage of BrdU/PSA-NCAM cells back to the levels found in Sham-treated animals ($P < 0.05$, Fig. 5B, compare α-TGFR and control ADX animals). No differences between treatments were observed in Sham-operated rats, suggesting that the antibody treatment had a specific effect on the BrdU/PSA-NCAM cell population affected by ADX ($P = 0.6$, Fig. 5B).

TGF-β increases neurogenesis and attenuates NSC proliferation in vitro

To obtain direct proof of the effects of TGF-β on NSC differentiation towards a neuronal phenotype, a culture of rat adult hippocampal NSC was incubated with different doses of TGF-β1 with or without the addition of serum. A physiological concentration of TGF-β1 (1 ng/mL) was able to increase the percentage of Tuj I+ cells even in the absence of serum (Fig. 6A–E). Importantly, this effect was blocked by the addition of a neutralizing antibody against TGF-β1 (Fig. 6E). In addition, the effects of TGF-β1 on NSC proliferation were evaluated. A minor, but statistically significant reduction in the percentage of BrdU-positive cells that were also PCNA-positive was detected in TGF-β-treated cells compared with untreated cells. Such a slight effect was abolished by coincubation with the TGF-β neutralizing antibody (Fig. 6F–H). The percentage of total BrdU-positive cells that were immunoreactive for PCNA was 54%, 45% and 55% for untreated, TGF-β-treated and TGF-β and anti-TGF-β-treated cells, respectively.

Discussion

In this study, we explored the possibility that the activation of microglial cells and the consequent expression of immune cytokines can modulate the proliferation and/or differentiation of NSC in adrenalectomized rats. We approached this issue using a sequential analysis. First, we confirmed the previously published effects of ADX on NSC proliferation and differentiation and additionally characterized the main cellular and molecular components of the new niche in the DG of ADX animals. Microglial activation was observed till stages 2 and 3 (but not stage 4, ED-1+) and this activation correlated with the degree of neurogenesis and NSC proliferation. Second, we identified a component of the new niche, TGF-β, an anti-inflammatory cytokine, as a candidate that contributes to the ADX-triggered, neurogenic effect and third, we showed that TGF-β was involved in promoting neurogenesis *in vivo* and was capable of doing so directly *in vitro*. Thus, we report here for the first time that an anti-inflammatory cytokine is pro-neurogenic in an environment of activated microglia

FIG. 3. Microglial activation in the GCL after ADX. (A) Immunofluorescence analysis showing *G. simplicifolia* isolectin-B4-positive cells (GSAI-B4 red) in the GCL after ADX treatment. Dotted line outlines the GCL. (B) Detailed photomicrograph of representative GSAI-B4-positive cells at different stages of activation (see Material and methods). Briefly, stage 1 cells were defined as resting microglia and had rod-shaped bodies with thin processes, stage 2 had an elongated morphology with very few and thick processes and stage 3 resembled macrophage morphology. (C) Double immunofluorescence for BrdU (green) and GSAI-B4 (red) of representative sections of ADX and Sham-operated animals. Some of the BrdU-positive cells colabelled with GSAI-B4 in ADX but not in Sham-operated animals. (D) Quantification of the total number of activated microglial cells (stage 2 and 3)/mm^3 DG for both treatments. ADX significantly induces microglial activation and proliferation (*$P < 0.05$, data were transformed; $\sqrt{x}$). (E) Correlation between microglial activation (stages 2 and 3) and neurogenesis. (F) Correlation between microglial activation and type 2 Nestin positive-cell proliferation (E) in ADX rats only. A positive correlation is observed (linear regression, $r^2 = 0.999$ and $r^2 = 0.96$, respectively). h, hilus; GCL, granule cell layer; ml, molecular layer. Scale bar, 20 μm.

FIG. 4. Analysis of cytokine expression in the hippocampus of ADX and Sham-operated animals. (A–D) Real Time RT-PCR for several cytokines expressed relative to β2-microglobulin mRNA expression (β2). (A) IL-1α mRNA expression; (B) IL-1β mRNA expression; (C) TGF-β1 mRNA expression. ADX significantly increases TGF-β1 expression in the hippocampus (*$P < 0.05$). Values are the mean ± SEM (Student's *t*-test. ADX $n = 4$, Sham $n = 5$). (D) Double immunohistochemistry analysis of TGF-β1 (brown) and GSAI-B4 (red). Black arrows indicate GSAI-B4-positive cells and white arrows indicate TGF-β stain. Dotted lines outline the subgranular cell layer of the DG. Note that both stains are localized mainly in the SGZ. (D′) Higher magnification of a different section showing a double-labelled cell for TGF-β and GSAI-B4. Asterisks indicates double-labelled cells. h, hilus; SGZ, subgranule cell layer. Scale bar, 20 μm. (E) Correlation between microglial activation and TGF-β1 expression in all rats. (F) Correlation between TGF-1 expression and neurogenesis in ADX rats. A positive correlation is observed (linear regression, $r^2 = 0.94$ and $r^2 = 0.99$, respectively).

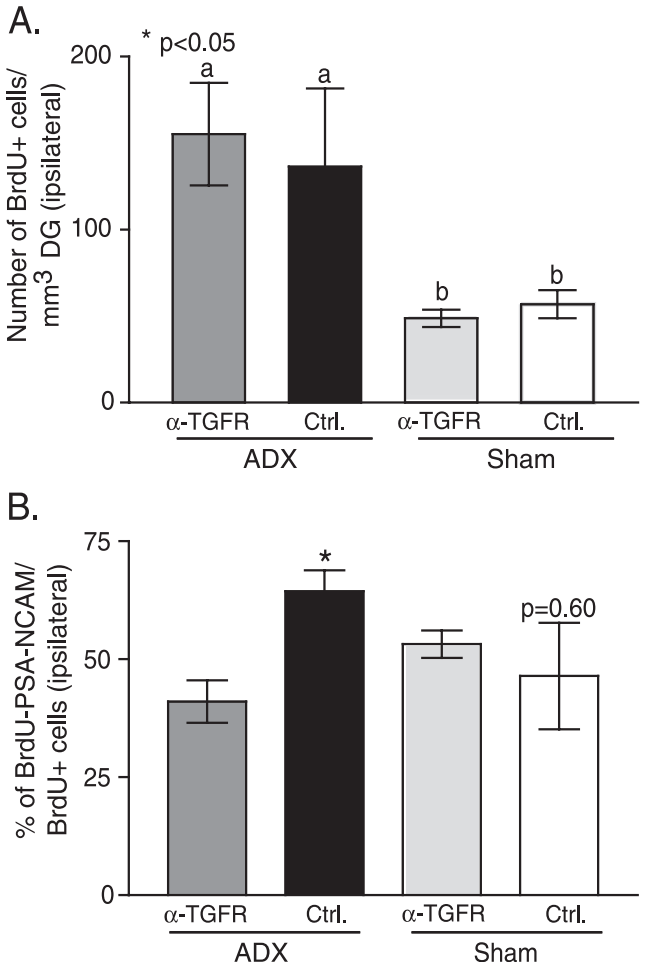

FIG. 5. Blockade of TGF-β receptor binding impairs neurogenesis induced by ADX. ADX and Sham-operated animals were injected in the DG with either an antibody against type II TGF-β receptor (α-TGFR) or control rabbit antiserum (Ctrl.) the day after surgery. (A) Number of BrdU-positive cells in the ipsilateral GCL/mm^3 DG in α-TGFR and control treated rats for both groups (ADX and Sham). There is no difference in the number of BrdU-positive cells between α-TGFR and control treatments for each group. The differences between ADX and Sham animals is still present (a^1b, *$P < 0.05$). (B) Quantification of BrdU/PSA-NCAM double-labelled cells in the ipsilateral GCL analysed by confocal *z*-scanning in ADX and Sham-operated animals. Blockade of type II TGF-β receptor in ADX rats results in decreased neurogenesis (*$P < 0.05$). Values are the mean ± SEM (A, ANOVA, Dunnett post test comparing all treatment with control, Sham Ctrl.; B, Student's *t*-test comparing α-TGFR and Ctrl. treatments in ADX and in Sham-operated animals; $n = 4$ for each treatment).

in vivo and is able to increase adult NSC differentiation to a neuronal phenotype by itself *in vitro*.

Our data are in line with previous reports showing increased apoptosis and cell proliferation in ADX animals compared to controls (Sloviter *et al*., 1989; Gould *et al*., 1992; Cameron & Gould, 1994; Cameron & McKay, 1999; Montaron *et al*., 1999). In addition, we provide further evidence that the population of proliferating cells consist of NSC (Nestin+), newborn neurons (PSA-NCAM) and microglial cells (GSA-BI). The previous reports determined neurogenesis by counting the number of cells in the subgranular cell layer that have incorporated radioactive thymidine or BrdU. We similarly determined that most of the proliferating cells (BrdU-positive) adopted a neuronal phenotype by studying the BrdU/PSA-NCAM population. In addition, we could show that, a higher, statistically significant percentage of the increased number of proliferating cells after ADX expressed the early neuronal marker PSA-NCAM compared with Sham animals (Fig. 1H).

A deeper analysis of the different Nestin-positive cells was performed to identify further the subpopulation of NSC that responded to the change produced in their environment by the lack of GC. We have classified Nestin-positive cells by their morphology according to Kemperman and colleagues (Kronenberg *et al*., 2003). The population of Nestin-positive cells that increased during ADX has similar morphological characteristics as the type 2 cell described by that group (Kronenberg *et al*., 2003). This subset of cells seems to have a higher proliferating index and starts to be committed to a differentiated phenotype, consistent with the increment in their numbers we observed in ADX animals. Thus, we identified an increase in a subset of Nestin-positive cells after ADX with similar morphological characteristics as the subset that expands under other stimuli such as running (Kronenberg *et al*., 2003; Kempermann *et al*., 2004). In conclusion, these data support the hypothesis that this subtype of Nestin-positive cells could be one that proliferates under a variety of neurogenic stimuli.

In addition to their action on neurons in the DG, GC are well known as regulators of cytokine synthesis in the periphery and the central nervous system (Rothwell & Hopkins, 1995; Besedovsky & del Rey, 1996; Goujon *et al*., 1996). In parallel, neuronal cell death by apoptosis has been recently shown to activate microglial cells with a defined activation pattern that markedly differs from a full-blown inflammatory reaction (Perry *et al*., 2002). Microglial cells activated by apoptotic neurons typically go up to stage 3 of activation and do not express a macrophagic marker (ED-1) or pro-inflammatory cytokines (Cunningham *et al*., 2002; Depino *et al*., 2003). Their profile of cytokine expression is in total agreement with the definition of apoptotic cell death, during which inflammation should not occur (Fadok *et al*., 1998). Interestingly, these characteristics of microglial activation resemble the ones described in models of chronic neurodegenerative diseases such as prion's and Parkinson's disease (PD) (Cunningham *et al*., 2002; Depino *et al*., 2003). In the ADX model, where neuronal death is apoptotic, microglial cells were driven until stage 3 of activation but not stage 4, remaining negative for the macrophagic marker ED-1 at the early time points studied. In addition, key pro-inflammatory cytokines were either not detected (TNF-α) or not significantly induced (IL-1 α and β). On the other hand, TGF-β was clearly up-regulated in ADX rats. Levels of TGF-β expression correlated highly with microglial activation to stage 2 and 3, as seen in neurodegenerative diseases such as prion's disease (Cunningham *et al*., 2002). Interestingly, only TGF-β levels correlated almost perfectly to the amount of neurogenesis observed in ADX rats. Furthermore, immuno-blockade of TGF activity by the administration of a TGF receptor II antibody in the DG significantly reduced neurogenesis in that area. These data demonstrate that TGF-β is part of the neurogenic niche that is driving NSC towards a neuronal phenotype in our model. In addition, the data provide the first example of an anti-inflammatory cytokine that can be pro-neurogenic *in vivo*.

Recently, it has been shown that a pro-inflammatory environment could have anti-neurogenic effects in the brain (Monje *et al*., 2002; Vallieres *et al*., 2002; Ekdahl *et al*., 2003; Monje *et al*., 2003). Some of those studies pointed at IL-6, a pro-inflammatory cytokine, as a key mediator of these anti-neurogenic effects (Vallieres *et al*., 2002); (Monje *et al*., 2003). Our evidence expands the concept, as it suggests that the final contribution of the activated microglia to the pro- or anti-neurogenic niche will depend on the degree of activation and a balance between the pro- and anti-inflammatory cytokines produced. Stage 2–

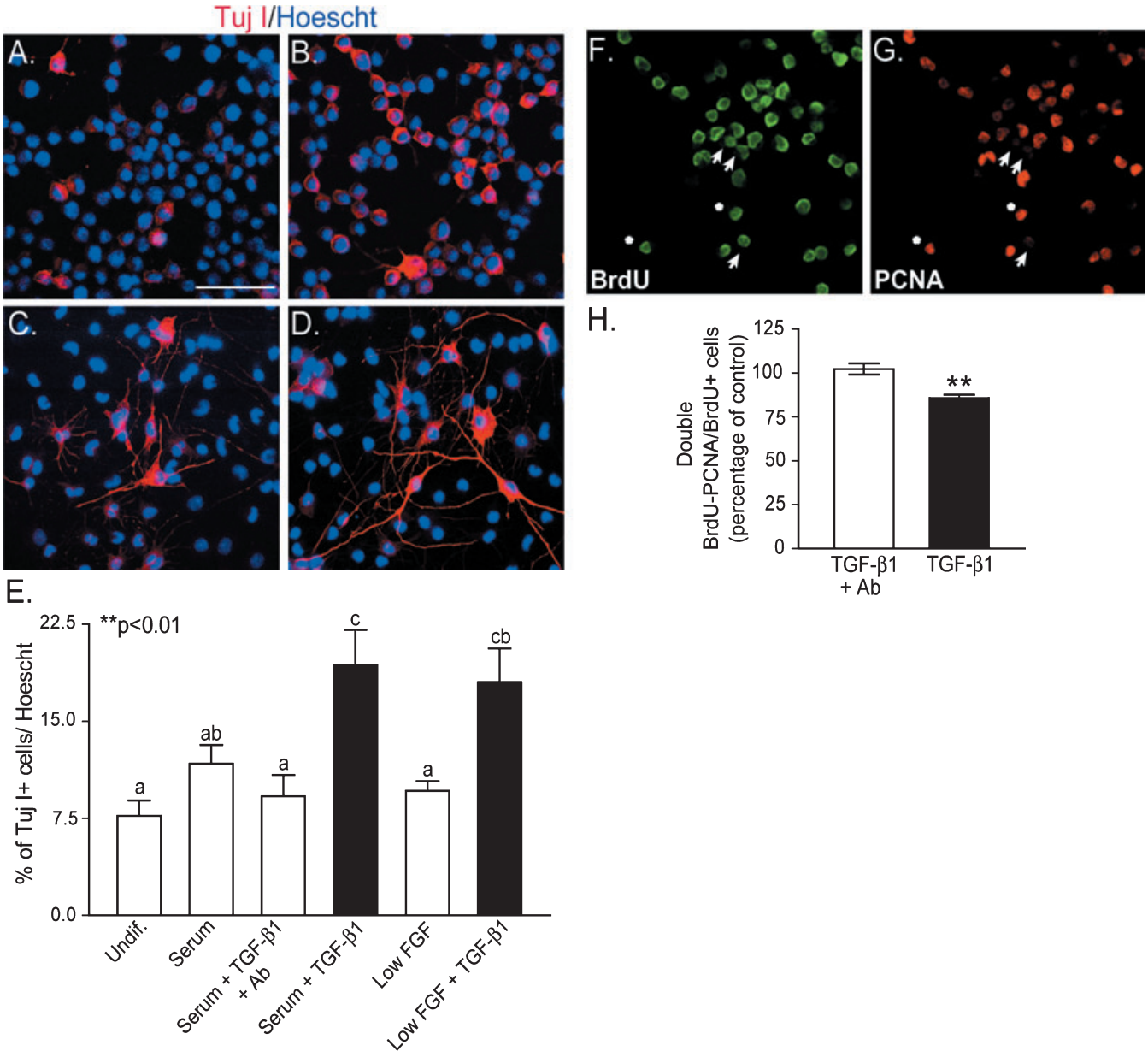

FIG. 6. TGF-β1 induces neurogenesis and slightly diminishes proliferation *in vitro*. (A–D) NSC cultures were stained for nuclear marker Hoescht (blue) and for type III β-tubulin (Tuj I, red) by immunofluorescence. Cells were treated with (B and D) or without (A and C) 1 ng/mL TGF-β1 in either standard medium containing serum (C and D) or standard medium with low FGF (A and B), as described in Material and methods. (E) Percentage of Tuj I positively stained cells over the total number of cells visualized with Hoescht for different treatments. As a control, 10 μg/mL of a neutralizing antibody against TGF-β1 was added to the culture. TGF-β1 increases neurogenesis in both medium conditions (a^1b^1c $^*P < 0.01$). (F and G) Pre-incubated NSC cultures with BrdU, stained for BrdU (green) and PCNA (red). A representative photomicrograph is shown. Arrows indicate double-labelled cells. Asterisks indicate BrdU single-labelled cells. NSC culture was pulsed for one hour with 20 nM BrdU and then treated with or without 5 ng/mL TGF-β1, as described in Material and methods. (H) Percentage of BrdU/PCNA double-labelled cells over the total of BrdU-positive cells treated with TGF-β1 alone or with TGF-β1 and a TGF-β1-neutralizing antibody. TGF-β1 significantly decreased proliferation ($^*P < 0.05$). Data are expressed relative to control (without TGF-β1). Values are expressed as the mean ± SEM (E, ANOVA, Tukey post test; H, Student's *t*-test. All treatments were performed in triplicate in three independent experiments). Scale bar, 50 μm.

3, ED-1-negative, activated microglial with TGF-β as a major cytokine in the environment could contribute to neurogenesis, whereas stage 4, ED-1-positive, fully activated microglia expressing IL-6 could promote inhibition of neurogenesis. Whether an increment in IL-6 could prevent the TGF-β neurogenic effect or the induction of TGF-β could affect the IL-6-anti-neurogenic potential remains to be investigated.

It is interesting to notice that the magnitude of the percentage of change in neurogenesis found in our model after ADX (Fig. 1H) is of a similar magnitude to the one found in a model of inflammation by LPS administration (Monje *et al.*, 2003). In our work, adrenalectomy caused a 10–20% increased in BrdU/PSA-NCAM-positive cells, which was blocked by TGF-β receptor antibodies (Figs 1 and 5). In that work, a 20% reduction in BrdU/doublecortin-positive, ED-1 negative cells was found in LPS-injected animals compared with controls (Monje *et al.*, 2003). In addition, the magnitude of the changes in neurogenesis *in vitro* are similar, although with opposite effects, between IL-6 and TGF-beta treated

NSC (Fig. 6 and Monje *et al*., 2003). Certainly, TGF-β can not be responsible to mediate all the ADX-dependent effects on neurogenesis and other ADX-related factors should also be acting. We propose that other endogenous factors that define the dentate gyrus as a neurogenic area may be acting to commit the proliferating NSC to a neuronal phenotype after ADX (Fig. 1). However, it is also clear that our *in vivo* evidence suggests that TGF-β contributed to the establishment of a pro-neurogenic environment in the dentate gyrus after ADX (Fig. 5). Our *in vitro* data further indicate that TGF-β is able to promote neurogenesis at physiological concentrations (1 ng/mL; Fig. 6).

TGF-β in not only a well-known anti-inflammatory cytokine but is a key molecule in development and cell cycle control (Roussa & Krieglstein, 2004). For example, TGF-β1 regulates melanocyte differentiation in mouse neural crest cells (Kawakami *et al*., 2002), is a key molecule in neural crest cell differentiation during development (Roussa & Krieglstein, 2004) and promotes neurogenesis in clusters of neural crest-derived multipotent progenitor cells that express TGF RII (Hagedorn *et al*., 2000). Importantly, TGF-β has been implicated in the development of dopaminergic neurons *in vitro* and *in vivo* in cooperation with Sonic hedgehog (Shh; Farkas *et al*., 2003). Shh is an important morphogen in development and has been implicated in the induction of NSC proliferation and differentiation (Lai *et al*., 2003; Alvarez-Buylla & Lim, 2004). In addition, TGF-β induces vascular endothelial growth factor (VEGF), a molecule involved in neurogenesis (Alvarez-Buylla & Lim, 2004). Whether TGF-β acts in cooperation with Shh, VEGF or other factors in neurogenesis, deserves future study.

A correlation was also found between the number of activated microglial cells and type 2 Nestin-positive cells ($r^2 = 0.998$). However, we have no evidence that TGF-β is affecting the cell cycle *in vivo* as in other cell systems (Roussa & Krieglstein, 2004). No correlation was found between TGF-β levels and NSC proliferation *in vivo*. In addition, TGF-blockade *in vivo* had no effect on NSC proliferation. Other authors have shown that neural stem cell proliferation is not always accompanied in a proportional fashion by neurogenesis. For example, in the manuscript by Monje and colleagues, irradiation-triggered inflammation caused reduced neurogenesis (Monje *et al*., 2003). This reduction in neurogenesis could be partially blocked by indomethacin, an anti-inflammatory compound. Importantly, this blockage of the inhibition of neurogenesis did not affect cell proliferation. Thus, as in our case, the effect of the factor under study (inflammation in their case or TGF-β in our case) on cell proliferation could be dissociated from neurogenesis. On the other hand, TGF-β slightly diminished NSC proliferation in culture. Our interpretation of this discrepancy is that TGF-β may have a subtle effect on NSC proliferation *in vitro* but additional, ADX-related factors may be mediating the proliferative effect *in vivo*.

In summary, these data highlight the functional role of microglial cells as components of a neurogenic niche in the brain. This work also supports the idea that activated microglial cells are not pro- or anti-neurogenic per se, but the balance between pro- and anti-inflammatory secreted molecules influences the final effect of this activation. Evidence is also presented that TGF-β, a known anti-inflammatory cytokine also involved in differentiation during development, can have a pro-neurogenic effect. Theoretically, this molecule could also be functional in modulating the inflammatory milieu towards a more neurogenic environment after transplantation of NSC in the brain. Finally, we provide another example of the functional relevance in CNS function of molecules traditionally studied in the immune system, such as immune cytokines.

Acknowledgements

We wish to thank Fabio Fraga for his assistance with animal handling. This work was supported by the Antorchas Foundation (F.P.), U.B.A. (F.P.), Rene Barón Foundation (F.P.), Carrillo-Oñativia fellowship (F.P.), the National Institute on Ageing (F.H.G.) and the National Institute of Neurological Disease and Stroke (F.H.G.). F.P. and C.F. are members of the research career of CONICET.

Abbreviations

ADX, adrenalectomized; DG, dentate gyrus; GC, glucocorticoids; NSC, neural stem cells; PB, phosphate buffer; PSA-NCAM, polysialic acid-neural cell adhesion molecule; TGF-β, transforming growth factor beta.

References

Alvarez-Buylla, A. & Lim, D.A. (2004) For the long run: maintaining germinal niches in the adult brain. *Neuron*, **41**, 683–686.

Besedovsky, H. & del Rey, A. (1996) Immune–neuro–endocrine interactions: facts and hypotheses. *Endocrine Rev.*, **17**, 1–39.

Besedovsky, H.O., del Rey, A., Sorkin, E. & Dinarello, C.A. (1986) Immunoregulatory feedback between interleukin-1 and glucocorticoid hormones. *Science*, **233**, 652–654.

Boche, D., Cunningham, C. & Gauldie, J. & Perry, V.H. (2003) Transforming growth factor-beta 1-mediated neuroprotection against excitotoxic injury *in vivo*. *J. Cereb. Blood Flow Metab.*, **23**, 1174–1182.

Cameron, H.A. & Gould, E. (1994) Adult neurogenesis is regulated by adrenal steroids in the dentate gyrus. *Neuroscience*, **61**, 203–209.

Cameron, H.A. & McKay, R.D. (1999) Restoring production of hippocampal neurons in old age. *Nature Neurosci.*, **2**, 894–897.

Cunningham, C., Boche, D. & Perry, V.H. (2002) Transforming growth factor beta1, the dominant cytokine in murine prion disease: influence on inflammatory cytokine synthesis and alteration of vascular extracellular matrix. *Neuropathol. Appl. Neurobiol.*, **28**, 107–119.

Depino, A.M., Earl, C., Kaczmarczyk, E., Ferrari, C., Besedovsky, H., Del Rey, A., Pitossi, F.J. & Oertel, W.H. (2003) Microglial activation with atypical proinflammatory cytokine expression in a rat model of Parkinson's disease. *Eur. J. Neurosci.*, **18**, 2731–2742.

Dinarello, C.A. (1996) Biological basis for IL-1 in disease. *Blood*, **87**, 2095–2147.

Ekdahl, C.T., Claasen, J.H., Bonde, S., Kokaia, Z. & Lindvall, O. (2003) Inflammation is detrimental for neurogenesis in adult brain. *Proc. Natl. Acad. Sci. USA*, **100**, 13632–13637.

Fadok, V.A., Bratton, D.L., Konowal, A., Freed, P.W., Westcott, J.Y. & H. (1998) Macrophages that have ingested apoptotic cells *in vitro* inhibit proinflammatory cytokine production through autocrine/paracrine mechanisms involving TGF-beta, PGE2, and PAF. *J. Clin. Invest.*, **110**, 890–898.

Farkas, L.M., Dunker, N., Roussa, E., Unsicker, K. & Krieglstein, K. (2003) Transforming growth factor-beta(s) are essential for the development of midbrain dopaminergic neurons *in vitro* and *in vivo*. *J. Neurosci.*, **23**, 5178–5186.

Ferrari, C.C., Depino, A.M., Prada, F., Muraro, N., Campbell, S., Podhajcer, O., Perry, V.H., Anthony, D.C. & Pitossi, F.J. (2004) Reversible demyelination, blood–brain barrier breakdown, and pronounced neutrophil recruitment induced by chronic IL-1 expression in the brain. *Am. J. Pathol.*, **165**, 1827–1837.

Gage, F.H. (2002) Neurogenesis in the adult brain. *J. Neurosci.*, **22**, 612–613.

Goujon, E., Parnet, P., Layé, S., Combe, C. & Dantzer, R. (1996) Adrenalectomy enhances pro-inflammatory cytokines gene expression, in the spleen, pituitary and brain of mice in response to lipopolysaccharide. *Mol. Brain Res.*, **36**, 53–62.

Gould, E., Cameron, H.A., Daniels, D.C., Woolley, C.S. & McEwen, B.S. (1992) Adrenal hormones suppress cell division in the adult rat dentate gyrus. *J. Neurosci.*, **12**, 3642–3650.

Hagedorn, L., Floris, J., Suter, U. & Sommer, L. (2000) Autonomic neurogenesis and apoptosis are alternative fates of progenitor cell communities induced by TGFbeta. *Dev. Biol.*, **228**, 57–72.

Kawakami, T., Soma, Y., Kawa, Y., Ito, M., Yamasaki, E., Watabe, H., Hosaka, E., Yajima, K., Ohsumi, K. & Mizoguchi, M. (2002) Transforming growth factor beta1 regulates melanocyte proliferation and differentiation in mouse neural crest cells via stem cell factor/KIT signaling. *J. Invest. Dermatol.*, **118**, 471–478.

Kempermann, G., Jessberger, S., Steiner, B. & Kronenberg, G. (2004) Milestones of neuronal development in the adult hippocampus. *TINS*, **27**, 447–452.
Kreutzberg, G.W. (1996) Microglia: a sensor for pathological events in the CNS. *TINS*, **19**, 312–318.
Kronenberg, G., Reuter, K., Steiner, B., Brandt, M.D., Jessberger, S., Yamaguchi, M. & Kempermann, G. (2003) Subpopulations of proliferating cells of the adult hippocampus respond differently to physiologic neurogenic stimuli. *J. Comp. Neurol.*, **467**, 455–463.
Lai, K., Kaspar, B.K., Gage, F.H. & Schaffer, D.V. (2003) Sonic hedgehog regulates adult neural progenitor proliferation *in vitro* and *in vivo*. *Nature Neurosci.*, **6**, 21–27.
Monje, M.L., Mizumatsu, S., Fike, J.R. & Palmer, T.D. (2002) Irradiation induces neural precursor-cell dysfunction. *Nature Med.*, **8**, 955–962.
Monje, M.L., Toda, H. & Palmer, T.D. (2003) Inflammatory blockade restores adult hippocampal neurogenesis. *Science*, **302**, 1760–1765.
Montaron, M.F., Petry, K.G., Rodriguez, J.J., Marinelli, M., Aurousseau, C., Rougon, G., Le Moal, M. & Abrous, D.N. (1999) Adrenalectomy increases neurogenesis but not PSA-NCAM expression in aged dentate gyrus. *Eur. J. Neurosci.*, **11**, 1479–1485.
Palmer, T.D., Makakis, E.A., Willhoite, A.R., Safar, F. & Gage, F.H. (1999) Fibroblast growth factor-2 activates a latent neurogenic program in neural stem cells form diverse regions of the adult CNS. *J. Neurosci.*, **19**, 8487–8497.
Paxinos, G. & Watson, C. (1986) *The Rat Brain in Stereotaxic Coordinates.* Academic Press, Orlando, FL.
Perry, V., Cunningham, C. & Boche, D. (2002) Atypical inflammation in the central nervous system in prion disease. *Curr. Opin. Neurol.*, **15**, 349–354.
Perry, V.H., Newman, T.A. & Cunningham, C. (2003) The impact of systemic infection on the progression of neurodegenerative disease. *Nature Rev. Neurosci.*, **4**, 103–112.
Rothwell, N.J. & Hopkins, S.J. (1995) Cytokines and nervous system. II. Actions and mechanisms of action. *TINS*, **18**, 130–136.
Roussa, E. & Krieglstein, K. (2004) Induction and specification of midbrain dopaminergic cells: focus on SHH, FGF8, and TGF-beta. *Cell Tissue Res.*, **318**, 23–33.
Sloviter, R.S., Valiquette, G., Abrams, G.M., Ronk, E.C., Sollas, A.L., Paul, L.A. & Neubort, S. (1989) Selective loss of hippocampal granule cells in the mature rat brain after adrenalectomy. *Science*, **243**, 535–538.
Vallieres, L., Campbell, I.L., Gage, F.H. & Sawchenko, P.E. (2002) Reduced hippocampal neurogenesis in adult transgenic mice with chronic astrocytic production of interleukin-6. *J. Neurosci.*, **22**, 486–492.